U-bent polymer optical fiber (POF) for *Escherichia coli* detection

A. R. A. RASHID[a,b*], A. A. N. HAKIM[a], N. YAHAYA[c], A. H. SURANI[a]
[a]*Applied Physics Programme, Faculty of Science and Technology, Universiti Sains Islam Malaysia, 71800, Nilai, Negeri Sembilan, Malaysia*
[b]*Frontier Materials Research Group (FMRG), Faculty of Science and Technology, Universiti Sains Islam Malaysia, 71800 Negeri Sembilan, Malaysia*
[c]*Food Biotechnology Programme, Faculty of Science and Technology, Universiti Sains Islam Malaysia, 71800, Nilai, Negeri Sembilan, Malaysia*

This research presents a plastic optical fiber (POF) based sensor to detect *Escherichia coli* at concentration of 10^3, 10^4, 10^5 and 10^6cfu/ml. The ESKA POF fiber composed of PMMA core and fluorinated polymer clad with refractive index of 1.49 and 1.41 respectively. Ethyl acetate solution was used to unclad 3 cm length of POF fibers and etched until 960 μm for all fiber sensors. U-shaped fiber with bending radius of 4 mm and 6 mm was developed by heating the fiber inside glass capillary tube. The penetration depth of the sensor is calculated by considering the internal and external curves of the U-shaped geometry. When tested with *E. coli*, fiber with bending radius of 4 mm shows a sensitivity of 9.5842 μW/RIU with slope linearity more than 97.82 % while, 6 mm produce sensitivity of 0.0353 μW/RIU with slope linearity 91.94 %. The performance of the sensor improved as the curvature radius decreased due to the light leaking and interact with the external medium. This can be concluded that by decreasing the bending radius, the penetration will be increased and thus affect the fiber's sensitivity.

(Received April 12, 2019; accepted April 9, 2020)

Keywords: Fiber optics, Biosensor, Evanescent wave, *E. coli*

1. Introduction

Clean and safe drinking water is essential for humans. However, water could be contaminated by the present of bacteria which effect on human health and causing several diseases. Microbiological test for drinking water should be taken seriously to reduce health risks. *Escherichia coli* as well as other type of coliform bacteria are commonly found in the soil. *E. coli* is considered as the species of coliform bacteria that have been used as the indicator of fecal pollution. Recently, the application of fiber optics as the sensing device arose over the years due to the its unique characteristics such as flexibility, high sensitivity and it is a low-cost sensor which can be developed. Many types of fiber optics based sensor is developed for pathogenic bacteria detection such as immunosensor based on the evanescent field [1], label-free detection technique of bacteria based on evanescent wave absorbance (EWA), principle of the sensor of sandwich immunoassay on the optical fiber surface and many more [2,3]. The application of fiber optics as medium of detections was widely developed such as detection the presence of the volatile organic compound [4], ultraviolet [5], alcohol detection [6] and uric acid [7]. The high evanescent field strength and penetration depth are crucial in order to obtain better sensitivity. The performance of bending fiber optics provided high strength detection of analytes. This work presents unclad POF sensor for *E. coli* detection for simple and low-cost sensor fabricated. The sensitivity obtained by the immersion of unclad POF in different refractive index of *E. coli* that depend on their concentration. The refractive index value of the surrounding medium influence the propagation of light inside the fiber [8]. Evanescent wave fiber-optic biosensors utilize evanescent wave detection techniques [9]. Electromagnetic waves propagate within an optical fiber by total internal reflection at the exposed surface and induces an evanescent electromagnetic field in any surrounding dielectric media. An evanescent field as in Fig. 1 is produced between cladding and core interface which cause exponential decayed shape as they become smaller from the core to the cladding.

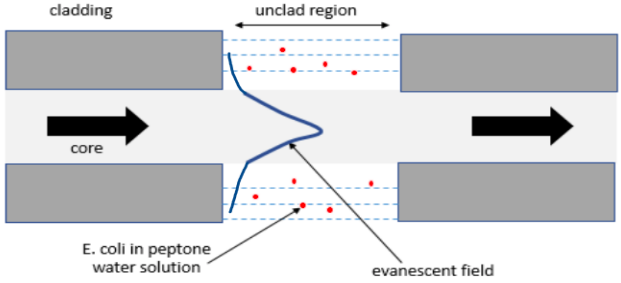

Fig. 1. Configuration of the evanescent field of uncoated fiber (color online)

2. Theory of U-Shaped Fiber

The penetration depth, d_p of an evanescent wave is very small in a straight fiber, but it can be notably increased by bending the fiber by forming to the U-shape geometry [10-11]. Thus, U-shaped geometry enhances the sensitivity of the fiber probe [12-13], notably chosen over the straight fiber in sensing application. The presentation of U-shaped POF is shows in Fig. 2, where the skewness angle is taken into account in the analysis. When the tapered region of the fiber is created, the mathematical solution of the wave equation is used to analyze [14]. The penetration depth of the fiber can be calculated as shown in the following Eq. (1) where λ is the vacuum wavelength of the light launched into the fiber, n_1 and n_2 are the refractive index of the core and cladding respectively. θ_c is critical angle in the sensing region with respect with the normal to the core-cladding interface, θ is the angle of the wave with the normal to the core-cladding interface, and θ_ϕ is the skewness angle [15].

$$d_p = \frac{\lambda}{2\pi n_1 (cos^2\theta_C - cos^2\theta sin^2\theta_\phi)^{1/2}} \quad (1)$$

The analysis of the skewness can be split depending on whether the light interacts with the outer or the inner surface. In the former case, the skewness angle of outer surface changes from ϕ_1 to ϕ_2 as shown in Eq. (2) and (3).

$$\phi_1 = sin^{-1}\left[\left(\frac{R+h}{R+2\rho}\right)\frac{n_{cl}}{n_1}\right] \quad (2)$$

$$\phi_2 = sin^{-1}\left(\frac{R+h}{R+2\rho}\right) \quad (3)$$

where R is the bending radius of the fiber, ρ is the radius of the fiber core, and h is the height at the entrance of the bent region from the inner core-cladding interface. At the inner surface, the angle can be written as δ_1 as shown in Eq. (4) and δ_2 is equal to 90 °.

$$\delta_1 = sin^{-1}\left[\left(\frac{R+h}{R}\right)\frac{n_{cl}}{n_1}\right] \quad (4)$$

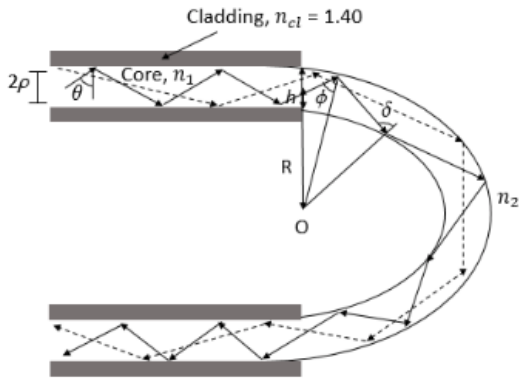

Fig. 2. Presentation of meridional ray in U-shaped POF

3. Materials and experimental set-up

The single colony of bacteria was cultured to study the sensitivity of the sensor upon exposure with *E. coli*. After a 24 hours incubation, the serial dilution is performed to obtain different concentration of bacteria. The clear broth turns cloudy indicate the growth of the *E. coli* in the broth culture as shown in Fig. 3. From broth culture, 1 ml of *E. coli* cells suspension were transferred into the 0.1% peptone water solution in the 9 ml tube to the required density, corresponding to 10^3, 10^4, 10^5, 10^6 bacteria to colony-forming units per milliliter with the most probably number per mL (MPN). The refractive index of the *E. coli* in peptone water is measured by using refractometer. The refractometer measures the degree of refraction that correlates them to the value of the refractive index.

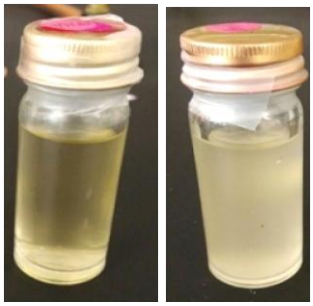

a) b)

Fig. 3. After 24 hours of incubation, (a) the clear broth (b) turns cloudy

For experimental setup, optical power meter and LED light source at wavelength of 650 nm was used. ESKA POF comprises of polymethylmethacrylate (PMMA) and fluorinated polymer as core and cladding having refractive indices of 1.49 and 1.41 respectively. For unclad region, unjacketed the POF fibers at length of 3 cm. The fiber was bent inside glass capillary tube to obtain U-shaped fiber geometry and heated in the oven for 5 minutes at the temperature of 100 °C. The fibers remain in U-shaped with radii curvature of 12 mm and 8 mm in diameter and immersed in ethyl acetate for 2 minutes to sensitize the core surface for evanescent wave-based sensing. The removal of certain length of cladding on the POFs can create the evanescent wave absorption in an external medium [16]. Then, the fibers are rinsed and immersed in deionized water at temperatures of 100 °C to neutralize the surface of the sensor part. The geometry of U-shaped fiber optics of etched fiber is shown in Fig. 4 while the experimental set up for the detection is shown in Fig. 5.

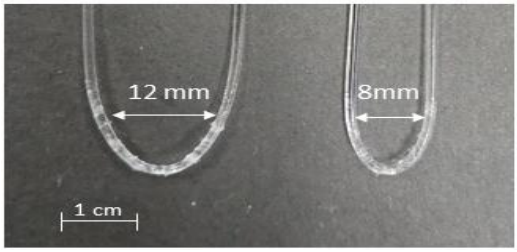

Fig. 4. The geometry of U- shape POF with diameter of 12 mm and 8 mm

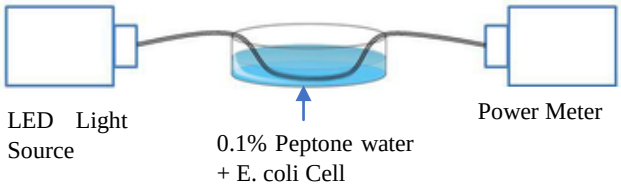

Fig. 5. The experimental setup of unclad U-shaped POF fiber (color online)

4. Result and discussion

The rod shape of gram-negative bacteria *E. coli* is observed from gram staining technique as shown in microscopic image in Fig. 6

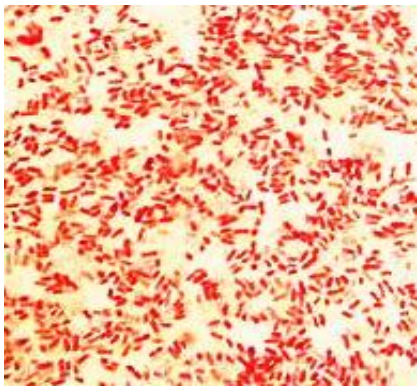

Fig. 6. The image of the pure sample of E. coli cells. The red color indicates gram-negative type of the bacteria (color online)

The refractive index of peptone water which contains different concentration of *E. coli* is determined by using refractometer. It shows a linear relationship between concentration and the refractive index of *E. coli* as shown in Fig. 7. The concentration of $10^3, 10^4, 10^5$ and 10^6 cfu/ml having the refractive indices 1.3322, 1.3326, 1.3328 and 1.3330 respectively. As the concentration of the *E. coli* rising, the value of refractive index also increased. The graph shows a linearly-dependent coefficient R^2 was 0.9888. This indicate that solutions sample used in the experiment can be recognized according to the solution accuracy [17].

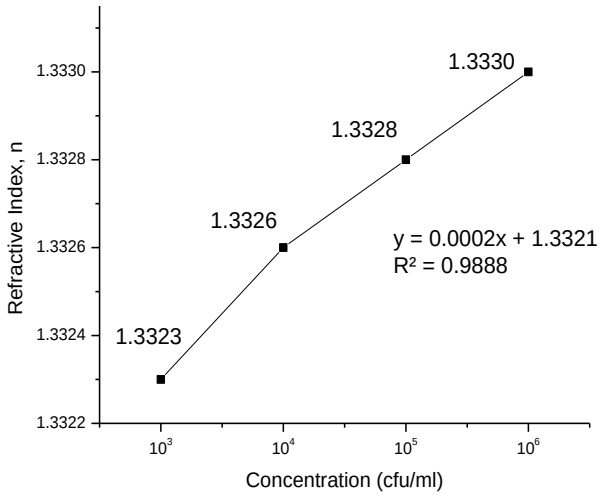

Fig. 7. The relationship between E. coli solution concentration and refractive index

In order to study the penetration depth of the unclad fibers, the concentration sample of *E. coli* with refractive index of 1.3330 is used and plotted based on the external curvature value as given in Eq. (1). The value of the penetration depth and numbers of reflections of 4 mm is calculated and shown in Table 1. The entrance height of light in the fiber is varied from 0 to 960 μm and calculated based on the skewness angle. At height, h=0, the value of penetration depth for external curvature is from 69.3567 nm to 69.3591 nm, while 69.3627 nm to 69.3760 nm for internal curvature. It shows that internal curvature has higher bending compare to external curvature, thus increase the penetration depth. Meanwhile, Fig. 8 shows the comparisons of penetration depth values versus height at the fiber's entrance for bending radius of 4 mm and 6 mm. From the graph, line of 4 mm of bending radius is steeper that show higher sensitivity compare to 6 mm. The fiber's sensitivity shows an improvement with reduction in bending diameter until it is equal to three times of the fiber diameter or less [8]. The performance of the refractive index sensor improved as the curvature radius decreased due to the light leaking and interact with the external medium [18-19]. The effect of the increasing refractive index and penetration depth of the evanescent field leads to higher sensitivity.

Table 1. Penetration depth and number of reflections at bending radius, R = 4 mm

h (μm)	Penetration depth, d_p (nm)				Numbers of Reflections, N			
	external curvature		internal curvature		external curvature		internal curvature	
	ϕ_1	ϕ_2	δ_1	δ_2	ϕ_1	ϕ_2	δ_1	δ_2
0	69.3567	69.3591	69.3627	69.3760	74.2104	63.6469	54.0341	38.0052
192	69.3574	69.3605	69.3653	69.3760	69.7751	59.2999	49.2629	38.0052
384	69.3586	69.3622	69.3695	69.3760	65.5874	55.0784	43.6924	38.0052
576	69.3597	69.3644	-	69.3760	61.6285	50.8222	-	38.0052
768	69.3611	69.3674	-	69.3760	57.7961	46.2201	-	38.0052
960	69.3627	69.3759	-	69.3760	54.0427	38.0052	-	38.0052

Fig. 9 shows the number of reflections in U-shape fiber. As the entrance height closer to the diameter of the fiber, the number of reflections decreased. The linearity value of 4 mm is higher than 6 mm bending radius which indicates higher number of reflections. The smaller bending radius produce higher reflection number due to bending loss of the fiber. It can be concluded that the lower bending radius results in higher penetration depth and number of reflections.

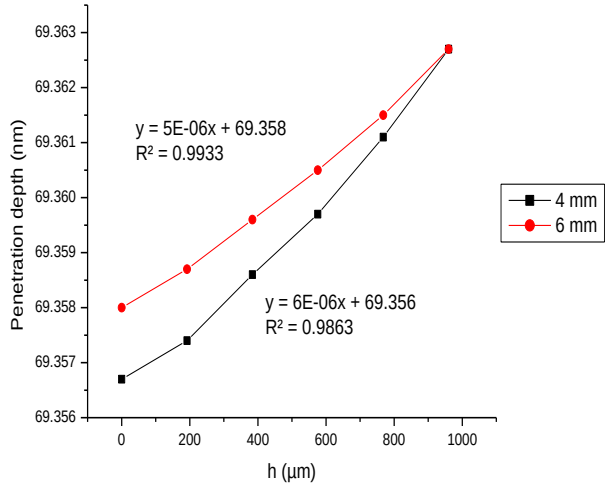

Fig. 8. Penetration depth of 4mm and 6 mm bending radius in immersion in 10^6cfu/ml of E. coli (color online)

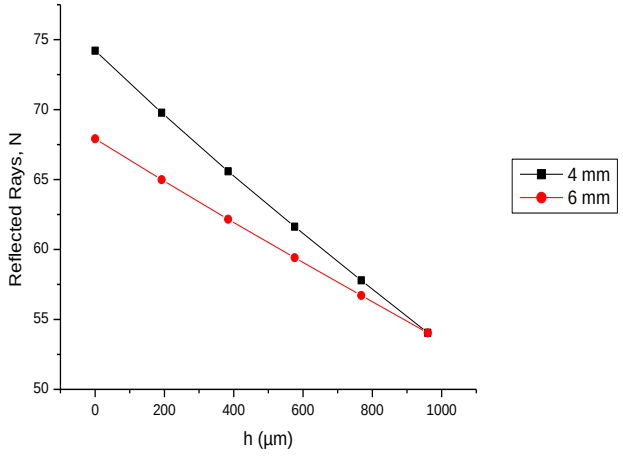

Fig. 9. Reflected ray of 4mm and 6 mm bending radius in immersion in 10^6cfu/ml of E. coli (color online)

Fig. 10 shows the power output ratio of U-shaped fiber under *E. coli* concentrations. Bending radius of 4 mm produces sensitivity of 9.5842 μW/RIU with slope linearity more than 97.82 % while, 6 mm fiber produce sensitivity of 0.0353 μW/RIU with slope linearity 91.94 %. It indicates smaller U-shaped fiber affect the sensitivity of detection [20]. However, the curvature radius is not the only parameter to measure the sensitivity of the sensor because it also depends on the structural parameter of the fabricated sensor [21]. Fang et al. state that the smaller the bending radius, the higher the sensitivity of the sensor as well as the fiber's performance in terms of transmission loss and measurement accuracy [17]. When the cladding is removed, the light will interact directly with the analyte. Therefore, the output power of this fiber is an inversed function of the analyte's refractive index. The smaller the refractive index, the more modes the fiber supports. As the refractive index of the analyte increases, the fiber supports less and less modes until the refractive index reached that of the core. At that point the critical angle is 90°, which, in practical terms means that the fiber does not guide any light, the light rays will not respect the bends instead they will propagate toward the outside of the fiber [22].

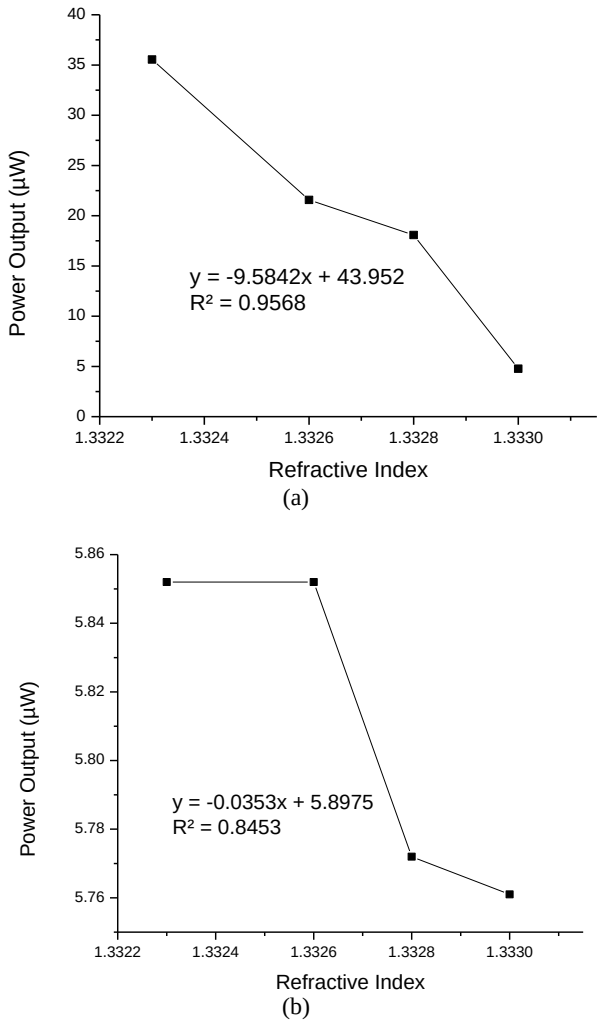

Fig. 10. Power output of uncoated POF with (a) 4 mm and (b) 6 mm bending radius under E. coli

EWAC of 4 mm of bending radius produces 0.03740 cm^{-1} to 0.06109 cm^{-1} at given length of 3 cm for unclad region. Similar with 6 mm bending radius, EWAC increases within 0.04144 cm^{-1} to 0.06939 cm^{-1} when the concentrations were varied from 10^3 to 10^6cfu/ml. Strong absorption of evanescent wave produced as the concentration and refractive index value increased. As

reported by Gupta et al., when the bending radius decreased, evanescent absorption coefficient and the sensitivity of the sensor will be increased [14]. When the fiber is immersed in the test solution, the evanescent field from the unclad region penetrates into the liquid and interacts with it. Strong evanescent wave absorption occurs on the modified part and it increases with increasing of concentration. An optical fiber sensor or biosensor usually detects the present of the analyte or cells around the fiber by the variation of refractive index [23].

5. Conclusion

It has been demonstrated that the application of U-shaped fiber can afford several advantages such as low-cost, ease of handling and simple technique for fabrication. The modification of the U-shaped geometry is suitable for detection of different concentration of *E. coli* by measuring the changes on the refractive index. Decrease in bending radius increases the value of evanescent absorption coefficient thus the sensitivity of the sensor is in agreement with the theoretical report. This label-free sensor allows to detect the differences of refractive index value of *E. coli* sample referring to the power output reading. Higher detection produces from 4 mm with a sensitivity 9.5842 μW/RIU compared to 0.0353 μW/RIU of 6 mm bending radius. Future work suggested to use antibody conjugate on coated fiber to capture *E. coli* on fiber's surface. Therefore, allowing a greater sensitivity of the developed sensor as lower number of bacteria could be captured [24]. Besides, adding more bending radius also suggested to increase the reliability of the result.

Acknowledgement

The authors would like to thank Faculty of Science and Technology, Universiti Sains Islam Malaysia (USIM) for guidance and support.

References

[1] D. M. C. Rodrigues, R. N. Lopes, M. A. R. Franco, M. M. Werneck et al., Sensors **17**(12), 2944 (2017).
[2] R. Bharadwaj, V. V. R. Sai, K. Thakare, A. Dhawangale, T. Kundu, S. Titus, P. Kumar, S. Mukherji, Biosens. Bioelectron. **26**(7), 3367 (2011).
[3] A. B. Socorro-Leranoz, D. Santano et al., Biosensors and Bioelectronics: X **1**, 100015 (2019).
[4] A. R. A. Rashid, P. S. Menon, S. Shaari, Optoelectron. Adv. Mat. **7**(11-12), 835 (2013).
[5] A. R. A. Rashid, P. S. Menon, S. Shaari, Journal of Nonlinear Optical Physics & Materials **22**(03), 1350037 (2013).
[6] S. Shaari, A. R. A. Rashid, P. S. Menon, N. Arshad, Advanced Science Letters **19**(5), 1306 (2013).
[7] A. R. A. Rashid, N. A. F. Shamsuri, A. H. Surani, A. A. N. Hakim, K. Ismail, Optoelectron. Adv. Mat. **13**(1-2), 63 (2019).
[8] A. Gowri, V. V. R. Sai, Sensors Actuators B. Chem. **230**, 536 (2016).
[9] C. S. Huertas, O. Calvo-Lozano, A. Mitchell, L. M. Lechuga, Front. Chem. **7**(724), 1 (2019).
[10] A. R. A. Rashid, W. M. Mokhtar, K. A. Dasuki, A. A. Ehsan, S. Shaari, Solid State Phenomena **268**, 413 (2017).
[11] P. K. Choudhury, T. Yoshino, Optik **114**(1), 13 (2003).
[12] J. Satija, N. S. Punjabi, V. V. R. Sai, S. Mukherji, Plasmonics **9**, 251 (2014).
[13] S. K. Srivastava, V. Arora, S. Sapra et al., Plasmonics **7**(2), 261 (2012).
[14] B. D. Gupta, H. Dodeja, A. K. Tomar, Opt. Quantum Electron. **28**(11), 1629 (1996).
[15] A. W. Snyder, J. D. Love, Optical Waveguide Theory; Springer: New York, NY, USA, 1984.
[16] P. S. Kumar, S. T. Lee, C. P. G. Vallabhan, V. P. N. Nampoori, P. Radhakrishnan, Optics Communications **214**(1-6), 25 (2002).
[17] Y. L. Fang, C. T. Wang, C. C. Chiang, Sensors (Switzerland) **16**(9), 1460 (2016).
[18] N. Jing, J. Zheng, X. Zhao, C. Teng, IEEE Sens. J. **15**(5), 2898 (2015).
[19] F. Sequeira, N. Cennamo, A. Rudnitskaya et al., Sensors **219**(11), 2476 (2019).
[20] D. M. C. Rodrigues, R. C. S. B. Allil, V. M. Queiroz, R. N. Lopes, A. Silva, M. Werneck, Proc. SPIE 9486, Advanced Environmental, Chemical, and Biological Sensing Technologies XII, 94860T (13 May 2015).
[21] N. Jing, J. Zheng, X. Zhao, C. Teng, Applied Optics **53**(34), 8145 (2014).
[22] G. Wandermur, D. Rodrigues, R. Allil, V. Queiroz, R. Peixoto, M. Werneck, M. Miguel, Biosens. Bioelectron. **54**, 661 (2014).
[23] R. Chachlani, M. Chhattopadhyay, M. E. Student, Int. Res. J. Eng. Technol. **4**(4), 2412 (2017).
[24] A. da S. Arcas, F. da S. Dutra, R. C. S. B. Allil, M. M. Werneck, Sensors **18**(2), 648 (2018).

*Corresponding author: affarozana@usim.edu.my